

# Mouse model of *Staphylococcus aureus*- and *Pseudomonas aeruginosa*-induced neutrophilic chronic rhinosinusitis

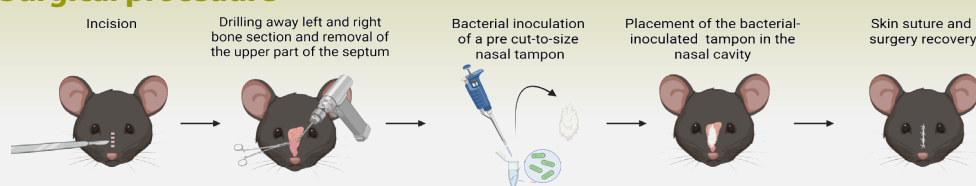
Alba Sánchez-Montalvo<sup>1,2</sup>, Aaron Ziani-Zeryouh<sup>1</sup>, Marylène Lecocq<sup>1</sup>, Brecht Steelant<sup>2</sup>, Sophie Gohy<sup>1,3,4</sup>, Peter Hellings<sup>2,5</sup>, Dominique Bullens<sup>2,6</sup>, Charles Pilette<sup>1,7</sup>, Valérie Hox<sup>1,8</sup>

Rhinology 63: 3, 352 - 362, 2025

<https://doi.org/10.4193/Rhin24.545>

## Mouse model of *Staphylococcus aureus*- and *Pseudomonas aeruginosa*-induced neutrophilic chronic rhinosinusitis

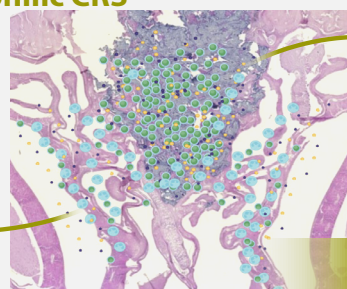
### Surgical procedure



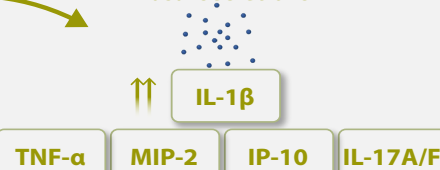
QR code shows detailed protocol + video of surgery

### Mouse model of non-eosinophilic CRS

- Bacteria
- Non-Type 2 inflammatory mediators
- Neutrophil



### Non-Type 2 inflammatory mediators in nasal secretions



*S. aureus* and *P. aeruginosa* are potent inducers of neutrophilic inflammation in mice. This model enables further study of non-eosinophilic CRS pathophysiology in vivo.

*Staphylococcus aureus* > *Pseudomonas aeruginosa* > *Streptococcus pneumoniae*

Sánchez-Montalvo A, Ziani-Zeryouh A, Lecocq M, et al. Rhinology 2025. <https://doi.org/10.4193/Rhin24.545>

RHINOLOGY  
Official Journal of the European and International Societies

### Abstract

**Background:** Chronic rhinosinusitis (CRS) is a highly prevalent upper airway disease. Its pathogenesis remains poorly understood, especially non-eosinophilic CRS. Currently, no validated mouse model exists to study disease mechanisms, indicating an important research gap. We aimed at establishing a reproducible mouse model of non-eosinophilic CRS to allow further research on its pathophysiology.

**Methodology:** Mice were infected with relevant bacteria for sinus disease via surgical insertion of a nasal tampon in their nasal cavity. Inflammatory features in sinus mucosa were evaluated after 4, 8 and 12 weeks on decalcified skulls by histology and immunohistochemistry and by cytopins and enzyme-linked immunoassay on nasal lavage.

**Results:** *S. aureus*-inoculated mice showed better survival than *S. pneumoniae*- and *P. aeruginosa*-inoculated mice. *S. aureus* and, to lesser extent, *P. aeruginosa* were still detectable in the nasal lavage up to 12 weeks. Mice with *S. aureus* and *P. aeruginosa*-induced CRS showed significant hypertrophy of the epithelium, neutrophilic infiltration and fibrosis in the sinus mucosa, with increased non-Type 2 cytokines in the nasal lavage.

**Conclusions:** *S. aureus* and *P. aeruginosa* are more potent inducers of neutrophilic inflammation than *S. pneumoniae* in mice. This model allows us to further study non-eosinophilic chronic rhinosinusitis pathophysiology in vivo.

**Key words:** bacteria, chronic rhinosinusitis, mouse models, neutrophils, non-eosinophilic inflammation

## Introduction

Chronic rhinosinusitis (CRS) is defined as an inflammation of nasal and paranasal sinus mucosa leading to two or more symptoms, one of which should be either nasal blockage/obstruction/nasal secretions, including headaches/facial pressure or pain and loss of smell. These symptoms last for over twelve weeks and are confirmed by endoscopy and/or imaging<sup>(1)</sup>. Affecting around 11% of the European population<sup>(2)</sup>, CRS severely impacts the quality of life of patients<sup>(3)</sup>, leading to significant loss of work productivity and health-care costs<sup>(4)</sup>.

In the most recent guidelines, CRS is classified according to its inflammatory profile<sup>(1)</sup>. Generally, in Western countries, patients with type 2 (T2) inflammatory profile often present with nasal polyp (NP) with mainly activated eosinophils and Th2 response, with increased IgE, IL-4, IL-5 and IL-13 in sinus tissue<sup>(5)</sup>. In patients with a non-T2 inflammatory profile, Th1 and/or Th17 responses are observed<sup>(6,7)</sup>, with mainly neutrophilic infiltration and increased IFN- $\gamma$ . In Western countries, NP are less likely to occur in this endotype<sup>(8)</sup>.

Environmental factors, genetic predisposition, anatomical differences and comorbid diseases are considered risk factors for CRS<sup>(9)</sup>. Defects in the sinonasal epithelium also play a key role in driving sinus inflammation<sup>(10)</sup>. Additionally, presence of certain pathogens, such as *Staphylococcus aureus*, have been linked to disease development<sup>(11)</sup>. Most research on CRS focuses on T2 CRS or eosinophilic CRS (eCRS). In contrast, studies on non-T2 or neutrophilic CRS (nCRS) are limited, despite it being the most frequent endotype<sup>(12)</sup>. Thus, its pathophysiology remains poorly understood.

Clinical research on CRS faces challenges due to genetic and environmental variability, driving interest in animal models to study this complex disease. Mouse models, despite differences from human airways, are valuable for studying immunological and respiratory diseases<sup>(13–15)</sup>. A mouse model for T2 eCRS based on experimental allergy and *S. aureus* enterotoxin B (SEB) exposure is widely accepted within upper airway research groups<sup>(16,17)</sup>. However, no established mouse model for nCRS exists, with very few reports published to date.

In this study we adapted and validated a mouse model reported by Jacob and colleagues in 2001 involving surgical introduction of a bacterial source combined with anatomical occlusion of the paranasal sinuses outflow tract<sup>(18)</sup>. Three bacterial strains relevant for sinonasal disease—*S. aureus*, *Streptococcus pneumoniae*, and *Pseudomonas aeruginosa*—were tested, with inflammatory features assessed at three time points. Inflammatory features were evaluated at three different time points. This resulted in a reliable and reproducible mouse model of nCRS that can help us

to gain insights into this disease entity.

## Materials and methods

### Experimental procedure to induce an experimental nCRS in mice

#### Animal model

C57BL/6NRJ male mice (7–8 weeks old, 25–30 g) were obtained from Janvier Labs and housed in an Animal Biosafety Level 2 (ABSL-2) facility, with agreement LA1230292. Mice were randomly divided into four groups: control (saline (NaCl 0.9%), n=28), *S. aureus* (n=36), *S. pneumoniae* (n=35), and *P. aeruginosa* (n=43). They were consecutively sacrificed four, eight and twelve weeks after surgery (Figure 1A). All animal experiments were performed in compliance with Ethical Committee guidelines (2021/UCL/MD/017, approval code 2000/13429.8).

#### Bacteria

Bacterial strains used were *P. aeruginosa* Vitroids™ (Sigma-Aldrich, VT000256), *S. aureus* Lenticules™ (Sigma-Aldrich, CRM06571M) and *S. pneumoniae* (ATCC®, 49619TM). Bacteria were cultured on sheep blood agar at 37°C overnight (*S. pneumoniae* required +5% CO<sub>2</sub>). They were then resuspended in saline, serially diluted to 1:10<sup>9</sup>, and 10 microliters of each dilution was plated and incubated for 24 hours. Colony counts were correlated to OD600nm to prepare solutions with 1×10<sup>9</sup> colony-forming units per milliliter (CFU/ml) according to optical density<sup>(19)</sup>.

#### Surgical procedure

The detailed protocol described in this article is published in protocols.io ([dx.doi.org/10.17504/protocols.io.rm7vzxwzgxg1/v2](https://dx.doi.org/10.17504/protocols.io.rm7vzxwzgxg1/v2)) and can be found as supplementary file within this article. Briefly, mice underwent micro-surgery (Figure 1B) using a stereomicroscope under anesthesia and analgesia administered according to safety recommendations<sup>(20,21)</sup>. An 8-mm midline incision was performed over the nasal dorsum to the snout and skin flaps were raised to expose the nasal bone. A 1.5-mm micro-drill (Medtronic) was used to drill the nasal bone over the nasal fossa and the upper part of the septum was removed. A pre-cut (4 mm x 1 mm x 1 mm) and sterilized nasal tampon (Medtronic) was soaked with ten microliters of a 10<sup>9</sup> CFU/ml solution of the corresponding bacteria or saline for controls. The tampon was placed in the nasal cavity, partially blocking the sinus outflow tracts, leaving sufficient space to breathe through the inferior meatus (Figure 1C). The skin was then sutured and mice were placed in a warm cage for recovery. Animal health and behavior were closely watched and monitored every day for one week and then four times a week until completion of the experiment to ensure well-being. If mice reached a score of non-well-being, mainly observed with respiratory distress, or lost more than 20% of their body weight, they were euthanized according to humane endpoints.

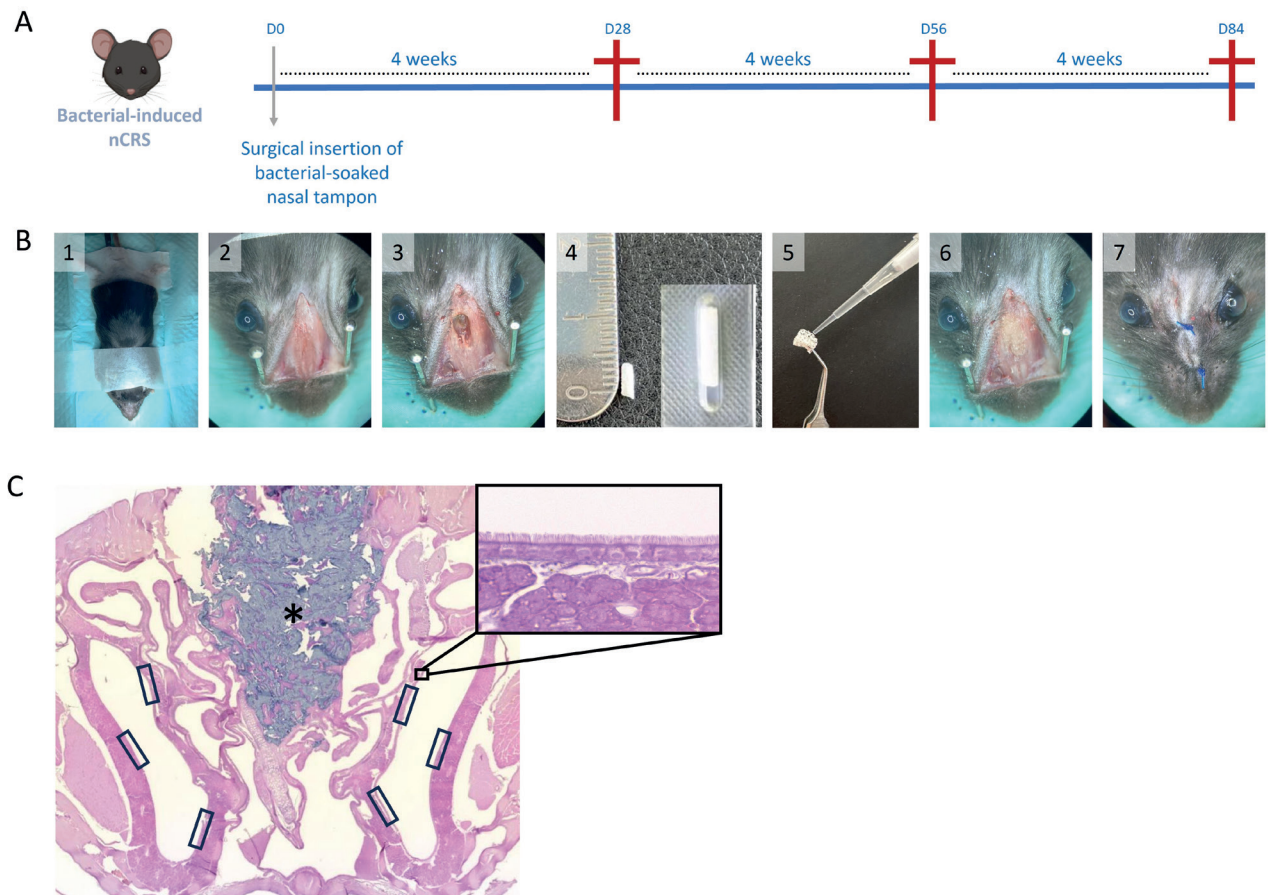


Figure 1. Experimental set up of the bacterial-induced nCRS mouse model and murine sinus anatomy. (A) Experimental design. (B) Overview of the surgical procedure. 1- The mouse is fixed in the surgical area. 2- Skin flaps are opened and 3- the nasal bones are drilled to expose the nasal mucosa. 4- A pre-cut to size sterile nasal tampon is 5- inoculated with a saline or bacterial solution and 6- inserted into the nasal cavity of the mice. Last, 7- skin is sutured with non-resorbable sutures. (C) Murine sinus anatomy, coronal sections, of a mouse inoculated with saline at four weeks post-surgery, H&E staining. Rectangles indicate the regions of the maxillary sinuses that were selected in each mouse to evaluate different histological features in a systematic way. Nasal tampon partially blocking the nasal cavity is indicated with an asterisk (\*). Zoom in shows the general state at the sinus epithelial layer, without noticeable signs of inflammation due to the presence of the nasal tampon inoculated with saline.

#### Sacrifice and sampling

Four, eight or twelve weeks after surgery, mice were euthanized. Blood was drawn from the inferior cava vein and serum was collected. Then, a tracheotomy enabled nasal lavage (NL) via inserting a 22G cannula (Versatus™ I.V Catheter) towards the choanae. One ml of saline was softly flushed in 200  $\mu$ L increments and recovered at the nostrils. Ten microliters were cultured, and the remaining NL fluid was centrifuged to separate cell pellets for cytopins, with the supernatant stored for further processing. Skulls were harvested, decapitated, cleaned of soft tissue, fixed in 4% formaldehyde and decalcified in Osteoral™ (RAL Diagnostics) for 5 days. The region containing paranasal sinuses was preserved, dehydrated, and treated according to standard paraffin-embedding procedures.

#### Bacterial culture

Ten microliters from NL were plated on sheep blood agar. Plates

were incubated at 37°C (5% CO<sub>2</sub> for *S. pneumoniae*) for 24 hours, after which bacterial colonies were identified and counted.

#### Cytopins from NL and inflammatory cell count

NL was collected as described above and centrifuged to separate the cell pellet. It was resuspended in 100 microliters of PBS and processed in a Thermo Shandon Cytospin at 500 rpm for 5 minutes. Cytopins were stained with the Kwik-Diff™ kit (Thermo Fisher Scientific), coverslipped and scanned using a Panoramic Scan II (3DHistech). Total inflammatory cells and neutrophils were counted with QuPath<sup>(22)</sup>. Results are presented as median  $\pm$  IQR.

#### Cytokine/chemokine measurements in NL

A custom mouse pro-inflammatory panel was used to detect multiple cytokines and chemokines in the NL fluid using the MSDTM V-PLEX technology (MSD, Rockville, MD) according to manufacturer's instructions: IFN $\gamma$ , (lower limit of detection

(LLD)= 0.07 pg/ml); IL-1 $\beta$  (LLD=0.081 pg/ml); IL-2 (LLD= 0.24 pg/ml); KC/GRO (LLD= 0.18 pg/ml); IP-10 (LLD= 0.328 pg/ml); IL-12p70 (LLD= 6.22 pg/ml); TNF $\alpha$  (LLD= 0.08 pg/ml); IL-33 (LLD= 0.28 pg/ml); IL-17A/F (LLD= 0.1 pg/ml); MIP-2 (LLD= 0.049 pg/ml). Results are presented as median  $\pm$  IQR.

### Histological and immunohistochemical analysis of the paranasal sinuses

Four  $\mu$ m paraffin sections were cut and stained. All slides were scanned using a Panoramic Scan II (3DHitech). Histological features were consistently analyzed in three regions of each maxillary sinus (lateral and medial areas; Figure 1C). Giemsa staining was performed to assess epithelial thickness, measured from basolateral to apical poles using Cytomine<sup>(23)</sup>. Results are presented as the median of 24 measurements/mouse  $\pm$  IQR. Subepithelial fibrosis was evaluated as collagen deposition via Sirius Red (SR) staining and analyzed with ImageJ based on the method described by Courtoy<sup>(24)</sup>. Results are presented as median of 6 measurements/mouse  $\pm$  IQR. Neutrophilic infiltration was analyzed through Ly6G-specific immunohistochemistry (IHC) using rat anti-mouse Ly6G (BD Bioscience, 551459) incubated for one hour at room temperature. Quantification was performed with QuPath<sup>(22)</sup> and expressed as the percentage of positive area. Results are presented as median of 6 measurements/mouse  $\pm$  IQR. To assess bacterial presence, IHC was performed with specific antibodies for *S. aureus* (PA17246, Thermo Scientific) and *P. aeruginosa* (ab68538, Abcam), incubated for one hour at room temperature.

### Statistics

Post-operative survival was analyzed using a Kaplan-Meier curve in GraphPad Prism 8.0. Statistical analyses of outcomes were also performed in Prism, with results presented as median  $\pm$  IQR. Statistical differences between experimental groups, comparing disease group to the control group of the same time point, were evaluated using the Kruskal-Wallis test, with Dunn's post-hoc control test for comparing multiple groups. A value of  $p < 0.05$  was considered significant. For cytokine/chemokine measurements, due to low sample sizes from dilution factor in NL, the Mann-Whitney U test was used to compare inoculated groups with controls, alongside the Kruskal-Wallis test to confirm trends. Results are indicated in different coloured stars on the graphs.

## Results

### Mice inoculated with *S. aureus* have a higher survival rate than *S. pneumoniae* and *P. aeruginosa*

No mice showed signs of local infection at the incision, nostrils, or eyes at any time point. Survival rates at 3 months post-surgery were significantly lower in mice with *S. pneumoniae*-induced CRS (80%) and *P. aeruginosa*-induced CRS (77%) compared to

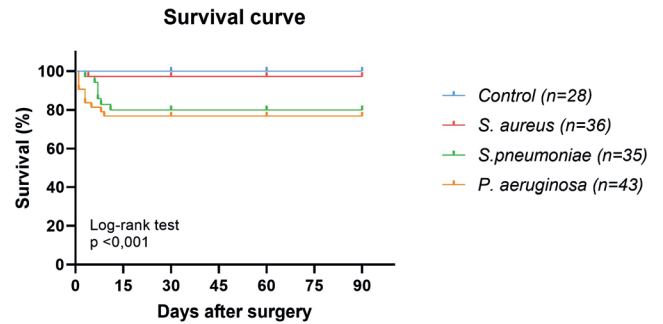


Figure 2. Survival of operated mice. Kaplan-Meier survival curves of mice with bacterial-induced neutrophilic CRS. The survival of mice (from the date of surgery until the end of the protocol) is compared by a standard log rank to test differences between controls with a saline-inoculated nasal tampon and the different bacterial-inoculated nasal tampon groups in the probability of a death.

*S. aureus* (97%) and saline controls (100%). None of the saline-inoculated mice showed high discomfort or mortality (Figure 2).

### *S. aureus* and *P. aeruginosa* remain detectable in nasal secretions up to 12 weeks post-operatively

Bacterial persistence in the nasal cavity was assessed 24 hours after seeding the NL in agar cultures. *S. aureus* was detected in 62% of mice at four weeks, 64% at eight weeks, and 45% at twelve weeks after surgery (Figure 3A). *S. pneumoniae* was detected in 33% at 4 weeks, 44% at 8 weeks, and 40% at 12 weeks after surgery (Figure 3A). *P. aeruginosa* was recovered in 50% of mice at 4 weeks, 45% at 8 weeks, and 30% at 12 weeks after surgery (Figure 3A). Cultures from saline-inoculated mice showed typical nasal commensals (data not shown).

*S. aureus* and *P. aeruginosa* were detected in the nasal tampon of inoculated mice by IHC up to twelve weeks post-surgery. These bacteria were also present in the maxillary sinuses but less abundant in the mucosa and only up to 4 weeks (Figure 3B). The histological presence of *S. pneumoniae* could not be assessed. No cross-contamination occurred between the bacterial groups.

### *S. aureus* and *P. aeruginosa* induce a more robust neutrophilic sinus inflammation than *S. pneumoniae*

Mice with *S. aureus*-induced CRS had significantly hyperplastic sinus epithelium at four weeks ( $p < 0.0001$ ), eight weeks ( $p < 0.01$ ), and twelve weeks ( $p < 0.01$ ) post-surgery (Figure 4A, C). Mice with *P. aeruginosa*-induced CRS showed significant epithelial hyperplasia at four weeks ( $p < 0.01$ ), eight weeks ( $p < 0.001$ ), and twelve weeks ( $p < 0.001$ ) post-surgery (Figure 4A, C). The epithelium of *S. pneumoniae*-induced CRS mice was significantly thicker at four weeks ( $p < 0.01$ ) and twelve weeks ( $p < 0.01$ ) post-surgery (Figure 4A, C).

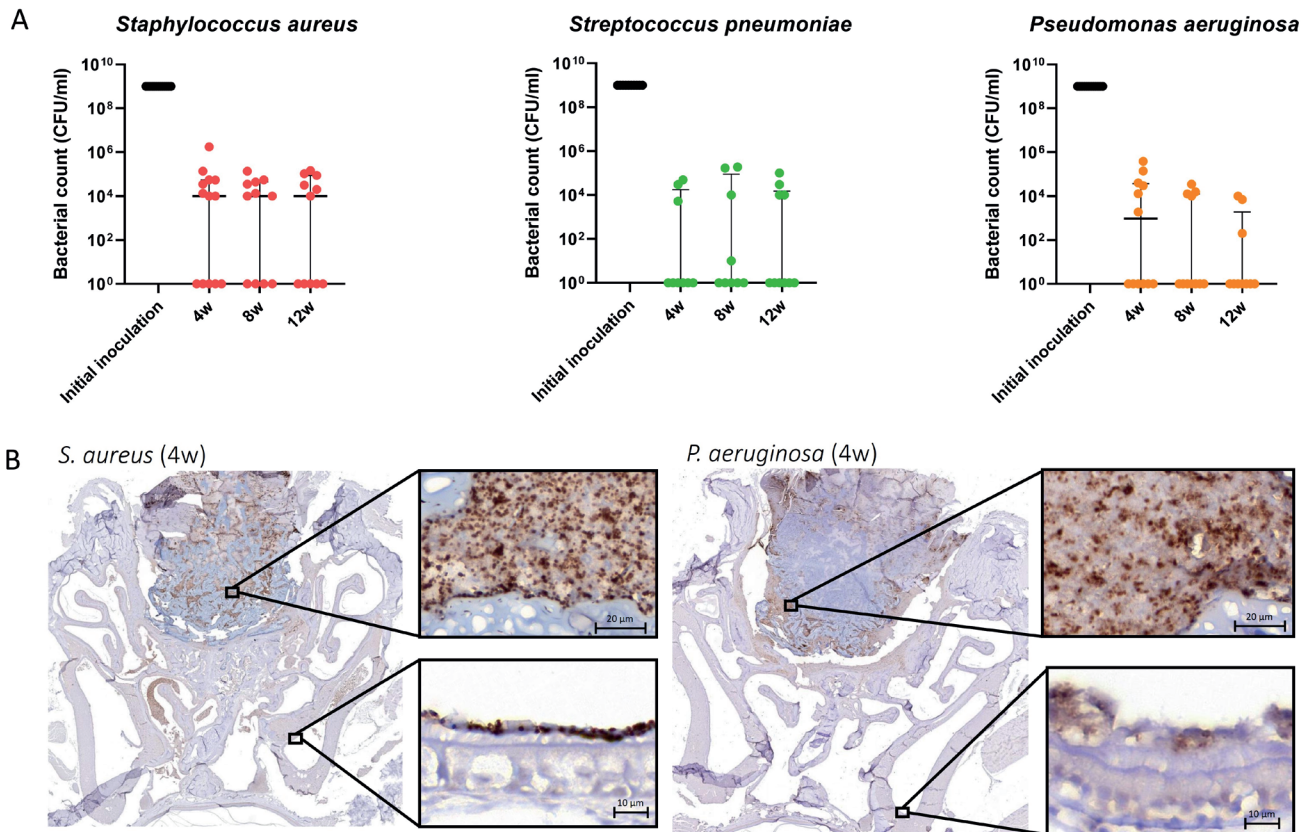


Figure 3. Bacterial cultures from NL at four, eight and twelve weeks after surgical inoculation. Bacterial count is expressed as CFU/ml. The initial inoculation refers to the bacterial solution with which the nasal tampon was inoculated during the surgical procedure. (A) *S. aureus* count (left), *S. pneumoniae* count (middle) and *P. aeruginosa* count (right). (B) Specific staining for *S. aureus* and *P. aeruginosa* four weeks after surgery. Graphs depict median  $\pm$  Interquartile range (IQR). n= 9-13 mice/group.

Subepithelial fibrosis was significantly higher in mice inoculated with *S. aureus* and *P. aeruginosa* at twelve weeks post-surgery (both  $p < 0.05$ ) with trends observed after four weeks in the *P. aeruginosa* ( $p = 0.06$ ) and *S. pneumoniae* groups ( $p = 0.09$ ) (Figure 4B, D).

Total inflammatory cells in NL of *S. aureus*-inoculated mice were increased four weeks ( $p = 0.06$ ) and especially twelve weeks ( $p < 0.01$ ) after surgery (Figure 5A). Neutrophils also increased at four weeks ( $p < 0.01$ ) and twelve weeks ( $p < 0.001$ ) after surgery (Figure 5B, C). In *P. aeruginosa*-inoculated mice, total inflammatory cells were significantly higher at twelve weeks ( $p < 0.001$ ) after surgery (Figure 5A) and neutrophils were increased at four weeks ( $p < 0.05$ ) and twelve weeks ( $p < 0.001$ ) after surgery (Figure 5B, C). *S. pneumoniae* also caused a significant increase in total inflammatory cells at twelve weeks ( $p < 0.05$ ) after surgery (Figure 5A), mainly neutrophils ( $p < 0.05$ ), with a visible trend to an increase at four weeks ( $p = 0.05$ ) after surgery (Figure 5B, C).

Significant neutrophilic influx was observed in the maxillary sinuses of *S. aureus*-inoculated mice at four weeks ( $p < 0.001$ ) and eight weeks ( $p < 0.01$ ) after surgery (Figure 5D, E). The same was

seen in *P. aeruginosa*-inoculated mice at four weeks ( $p < 0.01$ ) and eight weeks ( $p < 0.05$ ) after surgery (Figure 5D, E), with a slight reduction at twelve weeks for both bacterial strains. *S. pneumoniae*-inoculated mice showed significant neutrophilic infiltration at eight weeks ( $p < 0.05$ ) after surgery (Figure 5D, E).

#### Inoculation with *S. aureus* and *P. aeruginosa* led to increased nasal pro-inflammatory cytokine production

To explain the neutrophilic influx, non-T2 related cytokines were measured in NL and analyzed using the Mann-Whitney and Kruskal-Wallis tests (Figure 6).

IL-1 $\beta$  was significantly increased in *S. aureus*-inoculated mice at four weeks ( $p < 0.05$ ) after surgery, with a trend to persistent increase at twelve weeks ( $p = 0.052$ ) after surgery (Figure 6A). IL-1 $\beta$  was also increased in *P. aeruginosa*-inoculated mice at four ( $p < 0.05$ ), eight ( $p < 0.05$ ) and twelve weeks ( $p < 0.05$ ) after surgery (Figure 6A). It was also increased in *S. pneumoniae*-inoculated mice at four weeks ( $p < 0.05$ ) after surgery (Figure 6A).

TNF- $\alpha$  was significantly increased in *S. aureus*-inoculated mice at four weeks ( $p < 0.05$ ) after surgery (Figure 6B).

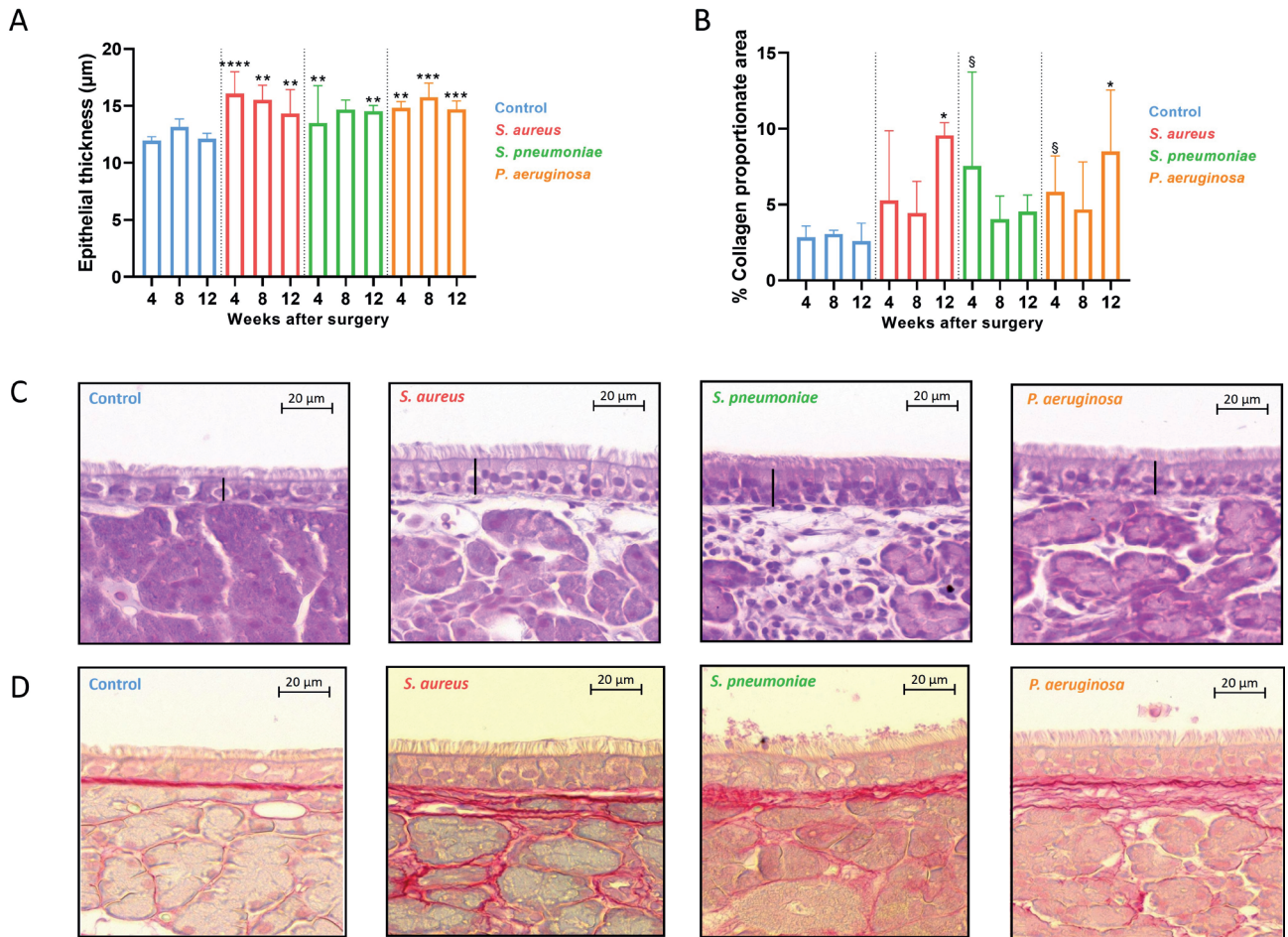


Figure 4. Histological changes in a mouse model of bacterial-induced nCRS. (A) Epithelial thickness measurements on H&E staining. Graph depicts median ( $\pm$ IQR) of 24 measurements per mouse performed by using Cytomine (23). (B) Subepithelial collagen deposition quantification on SR staining. Graph depicts median ( $\pm$ IQR) of 6 measurements per mouse performed by using ImageJ based on Courtoy<sup>(24)</sup>. (C) Representative pictures of the maxillary sinus epithelial layer, H&E staining. Black bars indicate how the epithelial thickness measurements were performed, from the base to the apical pole of the epithelial cells. (D) Representative pictures of the maxillary sinus epithelial layer, SR staining. Kruskal-Wallis with Dunn’s post-hoc control test for comparing multiple groups:  $\$p < 0.1$ ;  $*p < 0.05$ ;  $**p < 0.01$ ;  $***p < 0.001$ ;  $****p < 0.0001$  compared to the control group of the same time point.  $n = 9$ -13 mice/group for epithelial thickness; 3-5 mice/group for fibrosis quantification. Scale bar= 20  $\mu$ m.

Although the canonical Th1-related cytokine IFN- $\gamma$  was not detected in our samples because of high dilution in NL, changes in IP-10 (CXCL10), a chemokine secreted in response to IFN- $\gamma$  were found. Significantly increased IP-10 production by *S. aureus*-inoculated mice was found at twelve weeks ( $p < 0.05$ ) after surgery (Figure 6 C), with a trend to increased IP-10 production at eight weeks ( $p = 0.06$ ) after surgery (Figure 6C). A significant increase of IP-10 was found in *P. aeruginosa*-inoculated mice at eight weeks ( $p < 0.05$ ) after surgery (Figure 6C).

MIP-2 was significantly increased in *S. aureus*-inoculated mice at four weeks ( $p < 0.05$ ) and twelve weeks ( $p < 0.05$ ) after surgery (Figure 6D), with a trend to increased MIP-2 at eight weeks ( $p = 0.09$ ) after surgery (Figure 6D).

IL-17A/F showed a trend to increased levels in *S. aureus*-inoculated mice at eight weeks ( $p = 0.06$ ) and twelve weeks ( $p = 0.01$ ) after surgery (Figure 6E) and in *S. pneumoniae*-inoculated mice at eight weeks ( $p = 0.09$ ) after surgery (Figure 6E).

There were no significant variations in levels of KC/GRO (CXCL1) in any of the experimental groups at any of the time points studied (Figure 6F). Other cytokines that were tested, such as IFN- $\gamma$ , IL-12p70, IL-33 or IL-2, were not consistently upregulated upon bacterial inoculation.

### Discussion

The current study describes the validation of a robust mouse model of bacterial-induced nCRS, based on the combination of the introduction of a bacterial source in the nasal cavity and partial obstruction of the sinus outflow tract. We were able to

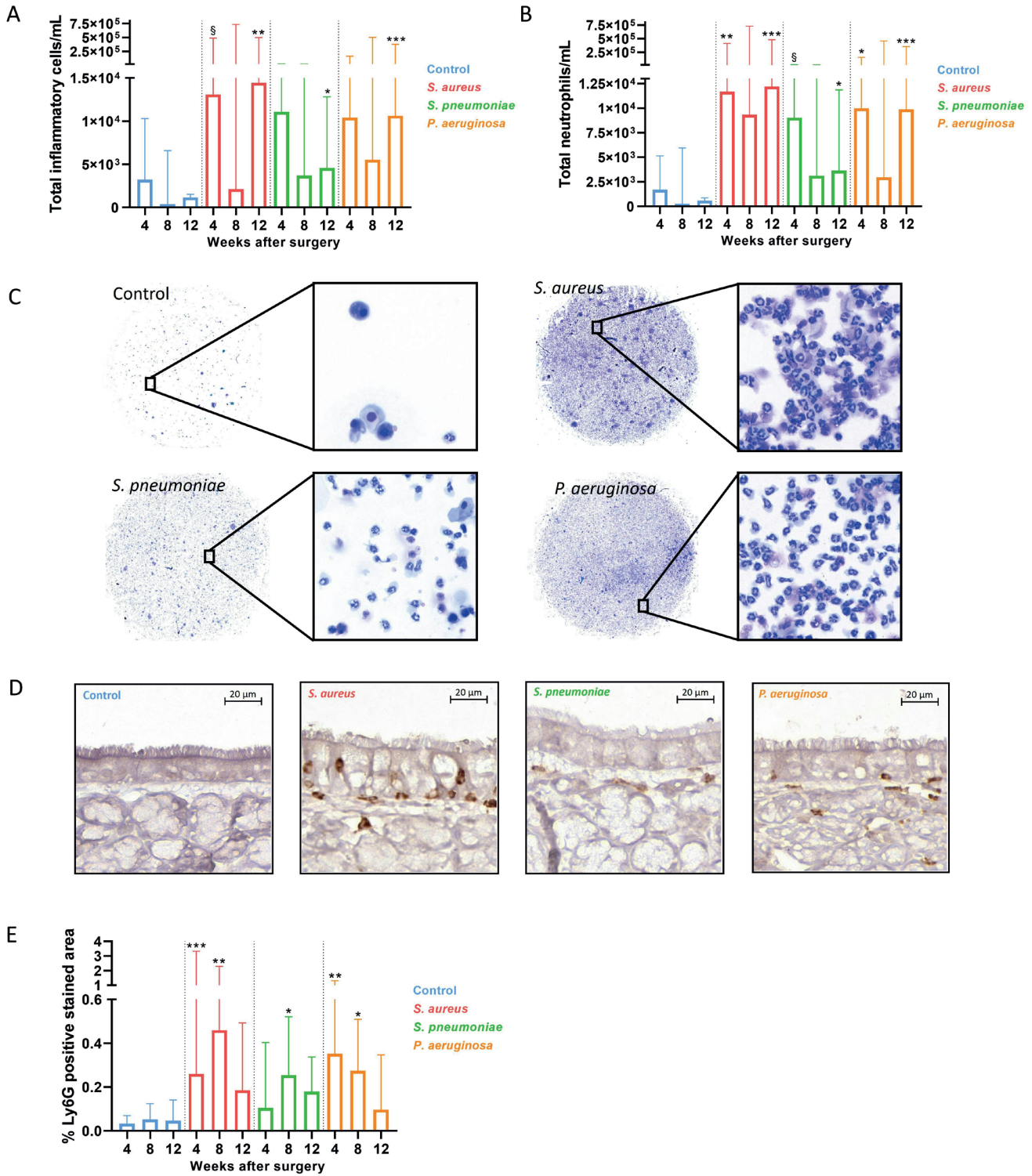


Figure 5. Inflammatory cell count in the NL and neutrophilic infiltration at the maxillary sinuses of a mouse model of bacterial-induced nCRS. (A) Total inflammatory cells/ml. Graph depicts median ( $\pm$ IQR). Counting was performed by using Cytomine<sup>(23)</sup>. (B) Neutrophils/ml. Graph depicts median ( $\pm$ IQR). Counting was performed by using Cytomine<sup>(23)</sup>. (C) Overview of the cytopins per group. (D) Histological sub- and intra-epithelial neutrophilic infiltration, Ly6G staining. (E) Ly6G staining quantification in tissue. Graph depicts median ( $\pm$ IQR) of 6 measurements per mouse performed by using Qupath<sup>(22)</sup>. Kruskal-Wallis with Dunn's post-hoc control test for comparing multiple groups: <sup>s</sup>p<0.1; \*p<0.05; \*\*p<0.01; \*\*\*p<0.0001 compared to the control group of the same time point. n= 9-13 mice/group.

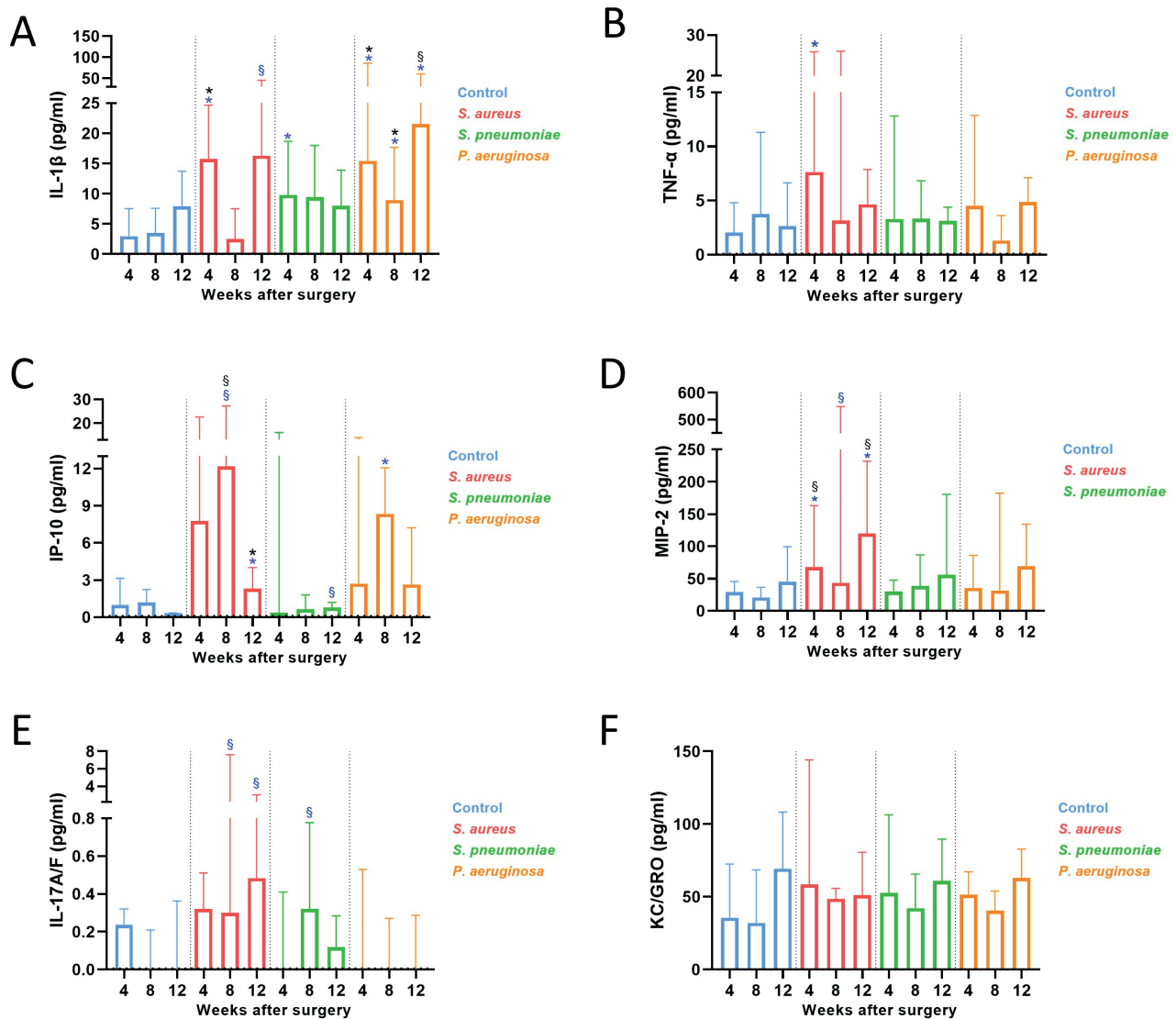


Figure 6. Cytokines and chemokines measurement by using MSD™ V-PLEX technology in the nasal lavage of a mouse model of bacterial-induced nCRS. (A) IL-1 $\beta$ , LLD= 0.081 pg/ml. (B) TNF- $\alpha$ , LLD= 0.08 pg/ml. (C) IP-10, LLD= 0.1 pg/ml. (D) MIP-2, LLD= 0.06 pg/ml. (E) IL-17A/F, LLD= 0.1 pg/ml. (F) KC/GRO, LLD= 0.18 pg/ml. Graphs depict median ( $\pm$ IQR). Kruskal Wallis with Dunn’s post-hoc control test for comparing multiple groups, in black \* $p$ <0.05; compared to the control group of the same time point. Because of low numbers of samples reaching the detection limit, Mann-Whitney U test was used, in blue, for comparing the inoculated mice and control mice at the corresponding time points: § $p$ <0.1; \* $p$ <0.05.  $n$ = 3-13 mice/group.

consistently induce general inflammatory features and a sinonasal neutrophilic influx up to 12 weeks after inoculation. *S. aureus* and *P. aeruginosa* have proven to be more potent inducers of persistent local neutrophilic inflammation than *S. pneumoniae*. This model might serve as a tool to study disease mechanisms of nCRS which remains currently a major research gap.

CRS is a frequent chronic airway disease with a high disease burden and socio-economic impact. Despite non-eosinophilic CRS being a very frequent endotype, especially in Asia, it remains under-researched and targeted treatments are lacking. Mechanical obstruction from anatomical abnormalities, mucosal

oedema and/or bacterial infection/colonization in biofilms have been postulated as potential drivers of the disease<sup>(25,26)</sup>, but confirming studies are still lacking. A validated mouse model replicating the human situation could be helpful in studying the disease but is currently not available.

Over recent decades, researchers have explored animal models involving bacterial inoculation to replicate human nCRS. In 2001, Jacob published a method in which a nasal tampon soaked with *Bacteroides fragilis* was surgically placed in the nasal cavity of mice, inducing a neutrophilic inflammation of the nasal septum and lateral wall of the nasal fossa four weeks after post-surgery

<sup>(18)</sup>. Later, another group extended the model to twelve weeks with *S. pneumoniae* to compare it with eosinophilic CRS <sup>(27)</sup>. Despite promising results, these two studies lacked critical methodological details and outcomes, and no further publications followed using this model. Because of our interest in nCRS pathophysiology, we decided to optimize this surgical protocol and test different bacteria and time points.

Human nCRS is histologically characterized by epithelial hyperplasia, fibrosis, and predominant mucosal influx by neutrophils <sup>(28)</sup>. These features could be observed in our mice inoculated with *S. aureus* and *P. aeruginosa*, resembling the neutrophil-driven inflammation and fibrosis seen in non-eosinophilic CRS in humans <sup>(12)</sup>, which involves pro-inflammatory cytokines as well as canonical Type 1 and/or Type 3 mediators <sup>(28,29)</sup>. Our model showed increased levels of IL-1 $\beta$ , with trends towards increases in TNF- $\alpha$ , neutrophil activator MIP-2, Type 1 chemokine IP-10, which is secreted in response to IFN- $\gamma$  <sup>(30)</sup>, and type 3 cytokine IL-17A/F, especially in mice with *S. aureus*-induced nCRS. However, significance was often lacking due to dilution from using 1 ml saline for nasal lavage, which led to an important dilution of nasal mediators that were often below detection limit (such as the typical Th1 cytokine IFN- $\gamma$ ). We therefore recommend using smaller NL volumes in case of specific study of local cytokines.

The strength of this paper lies in the fact that we provide guidance for a reproducible mouse model of nCRS, with the detailed surgical method published on protocols.io and included as supplementary material within this article. In our hands, a key challenge was positioning the nasal tampon within the nasal cavity to induce local inflammation with the lowest mortality, achieved by removing the upper part of the septum and positioning the tampon in the upper and middle meatus, allowing nasal breathing. Secondly, in this paper we also standardized sinus inflammation assessment, focusing on 3 fixed regions of the maxillary sinuses, since they are located at a significant distance of the nasal tampon compared to the ethmoidal sinuses, avoiding neutrophil influx due to the presence of a foreign object. Thirdly, to our knowledge, we are the first to describe the use of cytopins derived from NL, which proved to be a valuable tool to quantify sinonasal (neutrophilic) inflammation. Finally, we compared the effects of three different bacteria that are relevant in upper airway disease, at three different time points to come up with the most appropriate model. We chose *S. aureus* because, despite its well-known production of superantigens eliciting a T2 IgE mediated inflammatory response, its presence has also been linked to the enhancement of non-T2 pathways involving type 1 and 3 mediators <sup>(11)</sup>. *S. pneumoniae* was chosen because of its frequent link with acute rhinosinusitis <sup>(31)</sup>. *P. aeruginosa* is a bacterium with a high pathogenic potential, which can be detected in the microbiome of certain severe CRS patients and

more frequently in those suffering from cystic fibrosis (CF), characterized by non-T2 sinonasal inflammation <sup>(32)</sup>. We found that both *S. aureus* and *P. aeruginosa* were the most potent inducers of local inflammation in comparison to *S. pneumoniae*, likely linked to the fact that *S. pneumoniae* was more easily cleared from the nasal cavities by mice. Another explanation might be *S. aureus* and *P. aeruginosa* biofilm-forming capacities <sup>(33,34)</sup>, which are more structurally complex, more resistant to immune responses, as well as more adaptable to various environments compared to those from *S. pneumoniae* <sup>(33-36)</sup>. Our findings, therefore, suggest that this persistent sinonasal presence of bacteria with pathogenic capacity can be the driver for a long-lasting neutrophilic inflammation. We believe that this bacterial presence is more important than the mechanical obstruction of the sinus outflow tracts, since we also detected inflammatory changes in the sinuses that were not fully blocked and for which drainage pathway was still functional (data not shown). Of note, mice that were inoculated with *P. aeruginosa* showed a prolonged and more complex postoperative healing process, with bony overgrowth at the level of the drilling, which was also reflected in a higher mortality rate compared to *S. aureus*. So, while *P. aeruginosa* could be used to study more severe exacerbations of the disease and wound healing processes, we suggest using *S. aureus* as the preferred pathogen for this mouse model.

Our study has limitations that should be considered. The relatively small sample size per experimental group may limit the statistical power and the generalizability of the results. This may be in part related to the mortality rate observed per group, so further consideration of the chosen pathogen is necessary. Therefore, we advise to use *S. aureus* with regards to its neglectable mortality rate. Moreover, while animal models provide a controlled environment for studying disease mechanisms, we should be cautious on how we extrapolate findings to human pathology. Therefore, further research and validation of our optimized mouse model of bacterial-induced nCRS is needed. Also, the potential contribution of mixed microbial communities or biofilm formation, which are more representative of the human sinonasal environment, was not explored in this study. By addressing these factors, we aim to inspire further research that validates and builds upon our findings, particularly in identifying biomarkers and therapeutic targets and in better reflecting the complex etiology of human CRS for nCRS.

## Conclusion

Overall, this mouse model mimics human non-eosinophilic CRS and can be used to study the mechanisms driving inflammation and tissue damage observed in human nCRS. New insights in the pathophysiology of non-eosinophilic CRS may allow the identification of biomarkers and even new therapeutic targets. Additionally, this model could be used to test the efficacy of

existing and novel treatments for this condition. Finally, the model can serve to study the effects of different bacterial species on the sinus mucosa. We believe that it can lead to further and deeper understanding of this currently underexplored disease, allowing us to find novel treatment strategies for these patients that are now often left in the cold.

### Acknowledgements

We thank Caroline Bouzin and Aurélie Daumerie from the IREC Imaging Platform (2IP), for their valuable help concerning technical aspects of imaging acquisition and quantification.

### Authorship contribution

ASM: data collection, data analysis, experimental design, intellectual analysis, writing and reviewing of the manuscript. AZZ: data collection, data analysis, experimental design, intellectual analysis, writing and reviewing of the manuscript. ML: data collection, data analysis and reviewing of the manuscript. BS: intellectual analysis and reviewing of the manuscript. SG: intel-

lectual analysis and reviewing of the manuscript. PH: reviewing of the manuscript. DB: intellectual analysis and reviewing of the manuscript. CP: experimental design, intellectual analysis and reviewing of the manuscript. VH: experimental design, intellectual analysis, writing and reviewing of the manuscript. All authors have read and agreed to the published version of the manuscript.

### Conflict of interest

Nothing to declare.

### Funding

ASM is supported by an Aspirant fellowship of the Fonds National de la Recherche Scientifique (FNRS), Belgium. CP and SG are clinical researchers of the FNRS (grant 1.R016.20 and 1.R016.18), Belgium. VH is supported by a clinical post-doctoral mandate of the FNRS (grant 1R20221F), Belgium. The project was funded by an FRNS project grant (grant T011421F).

### References

- Fokkens WJ, Lund VJ, Hopkins C, et al. European Position Paper on Rhinosinusitis and Nasal Polyps 2020. *Rhinology*. 2020; 0(0): 1–464.
- Min HK, Lee S, Kim et al. Global Incidence and Prevalence of Chronic Rhinosinusitis: A Systematic Review. *Clin Exp Allergy*. 2025; 55(1):52-66.
- Khan A, Huynh TMT, Vandeplass G, et al. The GALEN rhinosinusitis cohort: chronic rhinosinusitis with nasal polyps affects health-related quality of life. *Rhinology*. 2019; 57(5): 343-351.
- Rudmik L. Economics of chronic rhinosinusitis. *Curr Allergy Asthma Rep*. 2017; 17(4): 20.
- Stevens WW, Peters AT, Tan BK, et al. Associations between inflammatory endotypes and clinical presentations in chronic rhinosinusitis. *J Allergy Clin Immunol Pract*. 2019; 7(8): 2812-2820.e3.
- Cao PP, Li H Bin, Wang BF, et al. Distinct immunopathologic characteristics of various types of chronic rhinosinusitis in adult Chinese. *J Allergy Clin Immunol*. 2009; 124(3): 478-84, 484.e1-2.
- Zhang N, Van Zele T, Perez-Novo C, et al. Different types of T-effector cells orchestrate mucosal inflammation in chronic sinus disease. *J Allergy Clin Immunol*. 2008; 122(5): 961-968.
- Tomassen P, Vandeplass G, Van Zele T, et al. Inflammatory endotypes of chronic rhinosinusitis based on cluster analysis of biomarkers. *J Allergy Clin Immunol*. 2016; 137(5): 1449-1456.e4.
- Min JY, Tan BK. Risk factors for chronic rhinosinusitis. *Curr Opin Allergy Clin Immunol*. 2015; 15(1): 1–13.
- Gohy S, Hupin C, Ladjemi MZ, Hox V, Pilette C. Key role of the epithelium in chronic upper airways diseases. *Clin Exp Allergy*. 2020; 50(2): 135-146.
- Delemarre T, De Ruyck N, Holtappels G, Bachert C, Gevaert E. Unravelling the expression of interleukin-9 in chronic rhinosinusitis: a possible role for *Staphylococcus aureus*. *Clin Transl Allergy*. 2020; 10(1): 41.
- Benjamin MR, Stevens WW, Li N, et al. Clinical characteristics of patients with chronic rhinosinusitis without nasal polyps in an academic setting. *J Allergy Clin Immunol Pract*. 2019; 7(3): 1010-1016.
- Al-Sayed AA, Agu RU, Massoud E. Models for the study of nasal and sinus physiology in health and disease: a review of the literature. *Laryngoscope Investig Otolaryngol*. 2017; 2(6): 398-409.
- Chamanza R, Wright JA. A review of the comparative anatomy, histology, physiology and pathology of the nasal cavity of rats, mice, dogs and non-human primates. relevance to inhalation toxicology and human health risk assessment. *J Comp Pathol*. 2015; 153(4): 287-314.
- Leite-Santos F, Tamashiro E, de Andrade Batista Murashima A, Anselmo-Lima WT, Valera FCP. Which are the best murine models to study eosinophilic chronic rhinosinusitis? a contemporary review. *Braz J Otorhinolaryngol*. 2023; 89(6): 101328.
- Kim DW, Khalmuratova R, Hur DG, et al. *Staphylococcus aureus* enterotoxin B contributes to induction of nasal polypoid lesions in an allergic rhinosinusitis murine model. *Am J Rhinol Allergy*. 2011; 25(6): e255-261.
- Sánchez-Montalvo A, Lecocq M, Bouillet E, et al. Validation and shortcomings of the most common mouse model of chronic rhinosinusitis with nasal polyps. *Rhinology*. 2024; 62(4): 446-456.
- Jacob A, Faddis BT, Chole RA. Chronic bacterial rhinosinusitis: description of a mouse model. *Arch Otolaryngol Head Neck Surg*. 2001; 127(6): 657-664.
- Hung CS, Dodson KW, Hultgren SJ. A murine model of urinary tract infection. *Nat Protoc*. 2009; 4(8): 1230–1243.
- Gargiulo S, Greco A, Gramanzini M, et al. Mice anesthesia, analgesia, and care, part ii: anesthetic considerations in preclinical imaging studies. *ILAR J*. 2012; 53(1): E70-81.
- Buitrago S, Martin TE, Tetens-Woodring J, Belicha-Villanueva A, Wilding GE. Safety and efficacy of various combinations of injectable anesthetics in BALB/c mice. *J Am Assoc Lab Anim Sci*. 2008; 47(1): 11–17.
- Bankhead P, Loughrey MB, Fernández JA, et al. QuPath: open source software for digital pathology image analysis. *Sci Rep*. 2017; 7(1): 16878.
- Marée R, Rollus L, Stévens B, et al. Collaborative analysis of multi-gigapixel imaging data using Cytomine. *Bioinformatics*. 2016; 32(9): 1395-1401.
- Courtoy GE, Leclercq I, Froidure A, et al. Digital image analysis of picosirius red staining: a robust method for multi-organ fibrosis quantification and characterization. *Biomolecules*. 2020; 10(11): 1585.
- Hekiart AM, Kofonow JM, Doghramji L, et al. Biofilms correlate with TH1 inflammation in the sinonasal tissue of patients with chronic rhinosinusitis. *Otolaryngol Head Neck Surg*. 2009; 141(4): 448-453.
- Wu J, Jain R, Douglas R. Effect of paranasal anatomical variants on outcomes in patients with limited and diffuse chronic

- rhinosinusitis. *Auris Nasus Larynx*. 2017; 44(4): 417–421.
27. Wang H, Lu X, Cao PP, et al. Histological and immunological observations of bacterial and allergic chronic rhinosinusitis in the mouse. *Am J Rhinol*. 2008; 22(4): 343–348.
28. Cho SH, Kim DW, Gevaert P. Chronic rhinosinusitis without nasal polyps. *J Allergy Clin Immunol Pract*. 2016; 4(4): 575–582.
29. Boraschi D. What Is IL-1 for? The functions of Interleukin-1 across evolution. *Front Immunol*. 2022; 13: 872155.
30. Coperchini F, Chiovato L, Rotondi M. Interleukin-6, CXCL10 and infiltrating macrophages in COVID-19-related cytokine storm: not one for all but all for One! *Front Immunol*. 2021; 12: 668507.
31. Brook I. Microbiology of chronic rhinosinusitis. *Eur J Clin Microbiol Infect Dis*. 2016; 35(7): 1059–1068.
32. Tuli JF, Ramezanzpour M, Cooksley C, Psaltis AJ, Wormald P, Vreugde S. Association between mucosal barrier disruption by *Pseudomonas aeruginosa* exoproteins and asthma in patients with chronic rhinosinusitis. *Allergy*. 2021; 76(11): 3459–3469.
33. Peng Q, Tang X, Dong W, Sun N, Yuan W. A review of biofilm formation of *Staphylococcus aureus* and its regulation mechanism. *Antibiotics (Basel)*. 2022; 12(1): 12.
34. Tuon FF, Dantas LR, Suss PH, Tasca Ribeiro VS. Pathogenesis of the *Pseudomonas aeruginosa* biofilm: a review. *Pathogens*. 2022; 11(3): 300.
35. Domenech M, García E, Moscoso M. Biofilm formation in *Streptococcus pneumoniae*. *Microb Biotechnol*. 2012; 5(4): 455–465.
36. Palmer J. Bacterial biofilms in chronic rhinosinusitis. *Ann Otol Rhinol Laryngol Suppl*. 2006; 196: 35–39.

**Valérie Hox**  
Department of Otorhinolaryngology  
Cliniques Universitaires Saint-Luc  
Av. Hippocrate 10  
1200 Brussels  
Belgium

Tel: +32 2 764 1111  
Fax: +32 2 764 3703  
E-mail: valerie.hox@uclouvain.be

Alba Sánchez-Montalvo<sup>1,2</sup>, Aaron Ziani-Zeryouh<sup>1</sup>, Marylène Lecocq<sup>1</sup>,  
Brecht Steelant<sup>2</sup>, Sophie Gohy<sup>1,3,4</sup>, Peter Hellings<sup>2,5</sup>, Dominique Bullens<sup>2,6</sup>,  
Charles Pilette<sup>1,7</sup>, Valérie Hox<sup>1,8</sup>

<sup>1</sup> Pole of Pneumology, ORL (airways) and Dermatology (skin) (LUNS), Institute of Experimental and Clinical Research (IREC), Université Catholique de Louvain (UCLouvain), Brussels, Belgium

<sup>2</sup> Department of Microbiology, Allergy and Clinical Immunology Research Group, Immunology and Transplantation, KU Leuven, Leuven, Belgium

<sup>3</sup> Department of Pneumology, Cliniques Universitaires Saint-Luc, 1200 Brussels, Belgium

<sup>4</sup> Cystic Fibrosis Reference Centre, Cliniques Universitaires Saint-Luc, 1200 Brussels, Belgium

<sup>5</sup> Clinical Department of Otorhinolaryngology, Head and Neck Surgery, UZ Leuven, Leuven, Belgium

<sup>6</sup> Clinical Division of Paediatrics, UZ Leuven, Leuven, Belgium

<sup>7</sup> Department of Pulmonology, Cliniques Universitaires Saint-Luc, Brussels, Belgium

<sup>8</sup> Department of Otorhinolaryngology, Cliniques Universitaires Saint-Luc, Brussels, Belgium

**Rhinology** 63: 3, 352 - 362, 2025  
<https://doi.org/10.4193/Rhin24.545>

**Received for publication:**

December 13, 2024

**Accepted:** March 8, 2025

**Associate Editor:**

Michael Soyka

**This manuscript contains online supplementary material**

## SUPPLEMENTARY MATERIAL

 protocols.io Part of **SPRINGER NATURE**

Apr 04, 2025 Version 2

### Surgical procedure to develop a bacterial-induced neutrophilic nasal inflammation in mice V.2

DOI

[dx.doi.org/10.17504/protocols.io.rm7vzxwzgx1/v2](https://dx.doi.org/10.17504/protocols.io.rm7vzxwzgx1/v2)

Alba Sánchez Montalvo<sup>1,2</sup>, Aaron Ziani Zeryouh<sup>1</sup>, Marylène Lecocq<sup>1</sup>, Charles Pilette<sup>1,3</sup>, Valérie Hox<sup>1,4</sup>

<sup>1</sup>Pole of Pneumology, ORL (airways) and Dermatology (skin) (LUNS), Institute of Experimental and Clinical Research (IREC), Université Catholique de Louvain (UCLouvain), Brussels, Belgium;

<sup>2</sup>Department of Microbiology, Immunology and Transplantation, Allergy and Clinical Immunology Research Group, KULeuven, Leuven, Belgium;

<sup>3</sup>Department of Pneumology, Cliniques Universitaires Saint-Luc, 1200 Brussels, Belgium;

<sup>4</sup>Department of Otorhinolaryngology, Cliniques Universitaires Saint-Luc, Brussels, Belgium

PhD



**Alba Sánchez Montalvo**

Institut de Recherche Expérimentale et Clinique (IREC)

OPEN  ACCESS



DOI: [dx.doi.org/10.17504/protocols.io.rm7vzxwzgx1/v2](https://dx.doi.org/10.17504/protocols.io.rm7vzxwzgx1/v2)

**Protocol Citation:** Alba Sánchez Montalvo, Aaron Ziani Zeryouh, Marylène Lecocq, Charles Pilette, Valérie Hox 2025. Surgical procedure to develop a bacterial-induced neutrophilic nasal inflammation in mice. **protocols.io**

<https://dx.doi.org/10.17504/protocols.io.rm7vzxwzgx1/v2> Version created by **Alba Sánchez Montalvo**

**License:** This is an open access protocol distributed under the terms of the **Creative Commons Attribution License**, which permits unrestricted use, distribution, and reproduction in any medium, provided the original author and source are credited

**Protocol status:** Working

**We use this protocol and it's working**

**Created:** March 14, 2024

**Last Modified:** April 04, 2025

**Protocol Integer ID:** 126140

**Keywords:** Surgery, nasal inflammation, neutrophils, mouse model

**Funders Acknowledgements:**

Fonds de la Recherche Scientifique (FNRS)

Grant ID: Research Fellow [ASP]

## Disclaimer

**DISCLAIMER – FOR INFORMATIONAL PURPOSES ONLY; USE AT YOUR OWN RISK**

The protocol content here is for informational purposes only and does not constitute legal, medical, clinical, or safety advice, or otherwise; content added to [protocols.io](https://www.protocols.io) is not peer-reviewed and may not have undergone formal approval of any kind. Information presented in this protocol should not substitute for independent professional judgment, advice, diagnosis, or treatment. Any action you take or refrain from taking using or relying upon the information presented here is strictly at your own risk. You agree that neither the Company nor any of the authors, contributors, administrators, or anyone else associated with [protocols.io](https://www.protocols.io), can be held responsible for your use of the information contained in or linked to this protocol or any of our Sites/Apps and Services.

## Abstract

The present surgical procedure provides a step-by-step and detailed protocol with all the critical information to develop a bacterial-induced neutrophilic local inflammation in the nasal mucosa of mice. The protocol is a modified and optimized version of the work previously published by Jacob et al. in 2001. The procedure consists of exposing and drilling out the nasal bones and the upper part of the septum followed by the insertion of a bacterial-inoculated nasal tampon in the nasal cavity which remains in situ until sacrifice.

## The day before surgery

- 1 Prepare the chosen bacteria 1d
- 1.1 Culture the corresponding bacteria on sheep blood agar plates (BD, Biosciences 254071), according to their specific growth requirements. 
- 1.2 In our hands, bacteria strains used were *Pseudomonas aeruginosa* Vitroids™ (Sigma-Aldrich, VT000256), *Staphylococcus aureus* Lenticules™ (Sigma-Aldrich, CRM06571M) and *Streptococcus pneumoniae* (ATCC® 49619™). Overnight culture conditions were 37°C for *S. aureus* and *P. aeruginosa* and 37°C in 5% CO<sub>2</sub> for *S. pneumoniae*.
- 2 Prepare the nasal tampon 4h
- 2.1 In our hands, a Merocel pope ear wick (Medtronic, MI, USA) was cut at a dimension of 4 mm x 1 mm x 1 mm and sterilized by dry heat 100°C during 3h.

## Pre-surgery

- 3 Prepare and sterilize your instruments for the surgical procedure
- 3.1 Stereomicroscope (Motic SMZ-171)  
 1.5-mm microdrill (Medtronic, MI, USA)  
 Sterile fields (Hartmann Mediset®)  
 Temperature monitor (PhysioSuite® Kent Scientific Corporation)  
 15-mm scalpel blade  
 5.0 non-resorbable polypropylene sutures (Monosoft™, Covidien)  
 Scalpel  
 Forceps  
 Scissors  
 Needles  
 Gloves (CardinalHealth™ Protexis™ PI micro surgical gloves)  
 Eye drops (Ocry-gel, TVM)  
 Chlorhexidine digluconate (Hibidil® , Regent Medical).  
 Tape  
 IR lamp (IR100 Infrared lamp, MEDISANA®)  
 Ultrasonic bath (Clifton)

- Surgery platform
- 4 Prepare your bacterial solution 30m
- 4.1 From the bacterial cultures, take isolated colonies and prepare serial dilutions up to  $10^9$  CFU/ml in NaCl 0.9% and measure it with a spectrophotometer with a reference optical absorbance at 600nm ( $OD_{600nm} = 1$ ).
- 5 Administration of anesthesia and analgesia to the mouse 30m
- 5.1 Weight the mouse and administer general anesthesia accordingly: a mix of Xylazin (maximum 15mg/kg) and Ketamin (maximum 80 mg/kg) intraperitoneally.
- 5.2 Administer analgesia: Temgésic (maximum 0,05 mg/kg) subcutaneously.
- 6 Wait 15-20 minutes for the aesthesia and analgesia to do their effect before starting the surgical intervention.

### Surgical procedure 10m

- 7 Shave the snout over the intervention area and fix the mouse on a sterile field (Figure 1, A).
- 8 Monitor and maintain the intraoperative body temperature of the mouse during the procedure.
- 9 Disinfect the intervention area with Chlorhexidine digluconate and use eye drops to prevent eyes from drying.
- 10 Use a 15-mm scalpel blade to make a 8-mm midline incision over the nasal dorsum to the snout. Raise skin flaps laterally to expose the nasal bone (Figure 1, B).
- 11 Use a 1.5-mm microdrill to drill the nasal bone over the nasal fossa and remove the upper part of the septum. Be extremely careful not to drill completely the bucco-sinusal bone communication. Clear out any bleeding to prevent aspiration (Figure 1, C).
- 12 Inoculate the pre-cut nasal tampon with 10  $\mu$ L of the corresponding bacterial solution or saline for controls and carefully place it into the nasal cavity (Figure 1, D-F).

- 13 Suture skin flaps with 5.0 non-resorbable polypropylene sutures and dettach the mouse from the surgical field (Figure 1, G).
- 14 Place the mouse in a cage softly heated laterally by an IR lamp for recovery after surgery. Make sure the lamp is not too close or too far from the cage (Figure 1, H).

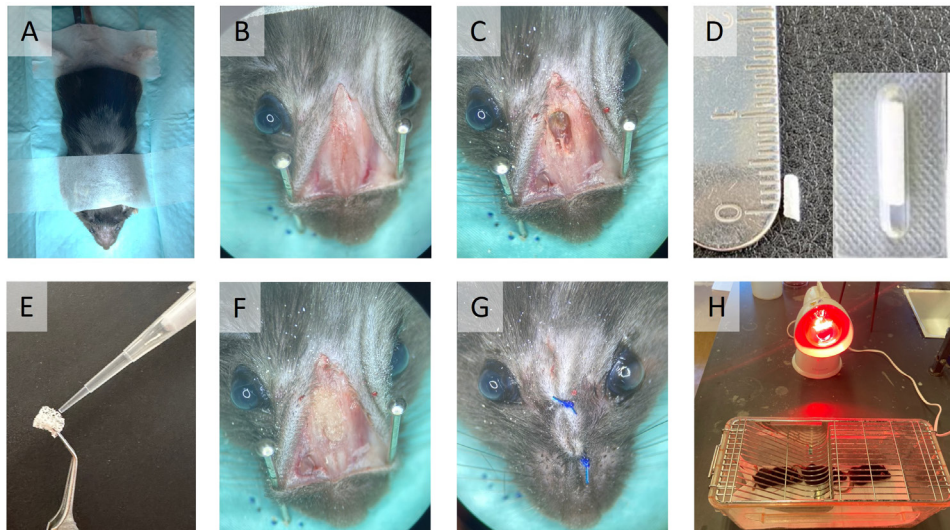
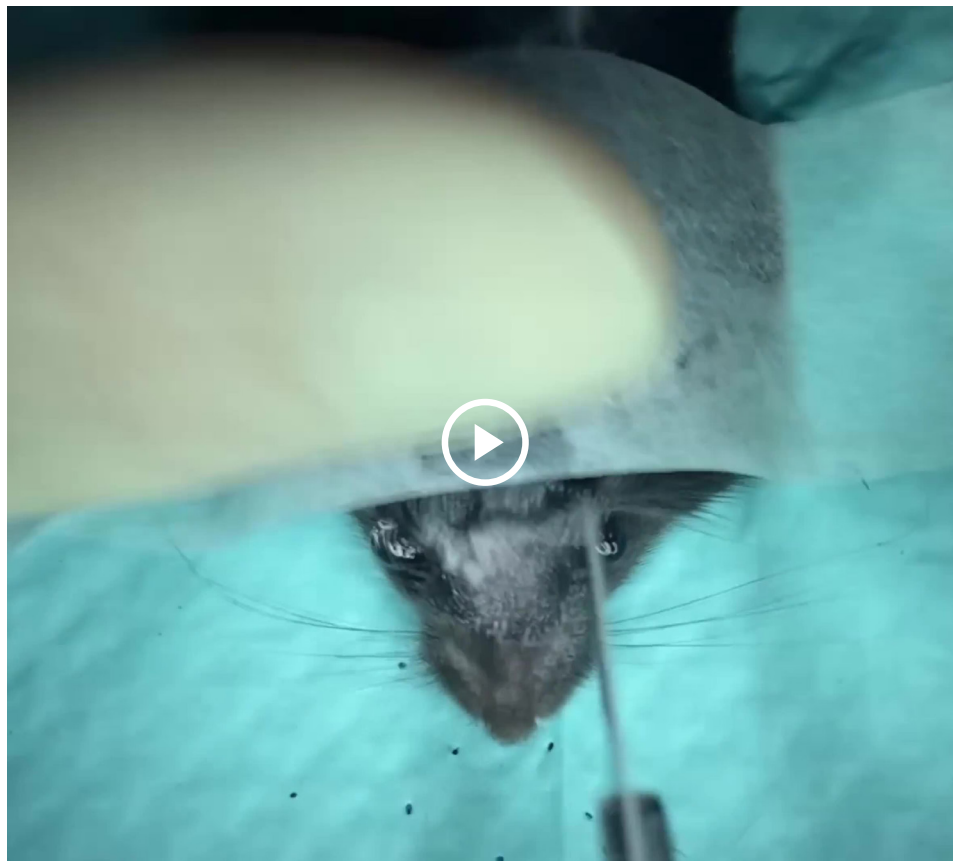


**Figure 1. Overview of the surgical procedure.** (A) The mouse is fixed in the surgical area. (B) Skin flaps are opened and (C) the nasal bones are drilled to expose the nasal mucosa. (D-E) A pre-cut sterile nasal tampon is inoculated with a saline or bacterial solution and (F) inserted into the nasal cavity of the mouse. Last, (G) skin is sutured with non-resorbable sutures and (H) the mouse is placed in a warm environment to recover.



**Video: surgical intervention.**

## Post-surgery care

- 16 Once awake and active, place the mouse into an ABSL-2 facility.
- 17 To overcome the possible post-operative pain, administer Temgésic (maximum 0,05 mg/kg) subcutaneously to the mice every 12h for 24h after surgery. 
- 18 Closely watch the animals every day for at least one week to ensure their well-being. According to humane endpoints, mice reaching a score of non well-being or losing more than 20% of their body weight must be euthanized. 

## Protocol references

Jacob A, Faddis BT, Chole RA. Chronic bacterial rhinosinusitis: description of a mouse model. Arch Otolaryngol Head Neck Surg. 2001 Jun;127(6):657-64. doi: 10.1001/archotol.127.6.657.